Inability to increase the neural drive to muscle is associated with task failure during submaximal contractions

Martinez-Valdes, Eduardo; Negro, Francesco; Falla, Deborah; Dideriksen, Jakob Lund; Heckman, C J; Farina, Dario

Published in:
Journal of Neurophysiology

DOI (link to publication from Publisher):
10.1152/jn.00447.2020

Publication date:
2020

Document Version
Accepted author manuscript, peer reviewed version

Inability to increase the neural drive to muscle is associated with task failure during submaximal contractions

*Eduardo Martinez-Valdes[1], *Francesco Negro[2], Deborah Falla[1], Jakob L. Dideriksen[3], Charles J. Heckman[4] , Dario Farina[5]

Affiliations

1. Centre of Precision Rehabilitation for Spinal Pain (CPR Spine), School of Sport, Exercise and Rehabilitation Sciences, College of Life and Environmental Sciences, University of Birmingham, Birmingham, UK
2. Department of Clinical and Experimental Sciences, Research Centre for Neuromuscular Function and Adapted Physical Activity "Teresa Camplani", Università degli Studi di Brescia, Brescia, Italy
3. Center for Sensory-Motor Interaction, Department of Health Science and Technology, Aalborg University, 9220, Aalborg, Denmark
4. Department of Physiology, Northwestern University, Chicago, IL, USA
5. Department of Bioengineering, Imperial College London, Royal School of Mines, London, UK

*Authors contributed equally to this work

Correspondence to:
Dario Farina
Department of Bioengineering, Imperial College London, London, UK.
Tel: +44 (0) 20 759 28 41387
Email: d.farina@imperial.ac.uk

Running title: Biphasic motor unit behaviour during fatigue
Keywords: Motor unit, fatigue, high-density surface electromyography, vastus medialis, vastus lateralis

Running title: Biphasic motor unit behaviour during submaximal fatiguing contractions

Competing Interests: The authors declare no competing financial interests.

ABSTRACT

We investigated changes in motor unit (MU) behaviour and vasti-muscle contractile properties during sustained submaximal fatiguing contractions with a new time-domain tracking technique in order to understand the mechanisms responsible for task failure. Sixteen participants performed a non-fatiguing 15s isometric knee-extension at 50% of the maximum voluntary torque (MVC), followed by a 30% MVC sustained contraction until exhaustion. Two grids of 64 surface electromyography electrodes were placed over vastus medialis and lateralis. Signals were decomposed into MU discharge-times and the MUs from the 30% MVC sustained contraction were followed until task failure by overlapping decomposition intervals. These MUs were then tracked between 50% and 30% MVC. During the sustained fatiguing contraction, MUs of the two muscles decreased their discharge rate until ~40% of the endurance time, referred to as the reversal time, and then increased their discharge rate until task failure. This reversal in firing behaviour predicted total endurance time and was matched by opposite changes in twitch force (increase followed by a decrease). Despite the later increase in MU firing rates, peak discharge rates at task failure did not reach the frequency attained during a non-fatiguing 50% MVC contraction. These results show that changes in MU firing properties are influenced by adjustments in contractile properties during the course of the contraction, allowing the identification of two phases. Nevertheless, the contraction cannot be sustained possibly due to progressive motoneuron inhibition/decreased excitability, as the later increase in firing rate saturates at a much lower frequency compared to a higher-force non-fatiguing contraction.

NEW & NOTEWORTHY

Motor unit firing and contractile properties during a submaximal contraction until failure were assessed with a new tracking technique. Two distinct phases in firing behaviour were observed, which compensated for changes in twitch area and predicted time to failure. However, the late increase in firing rate was below the rates attained in absence of fatigue, which points to an inability of the central nervous system to sufficiently increase the neural drive to muscle with fatigue.

INTRODUCTION

It is commonly assumed that during sustained submaximal contractions, muscle fatigue, defined as a reduction in the maximum force generation capacity of muscles, is a progressive phenomenon which develops from contraction onset and is associated to the same mechanisms during the contraction (Enoka and Duchateau 2008). This conclusion is based on previous observations that showed similar changes in central and peripheral electrophysiological properties during the entire duration of a task. For example, it has often been observed that the discharge rates of motor units progressively decrease from the beginning to the end of submaximal isometric contractions (Carpentier et al. 2001; Garland et al. 1994; McManus et al. 2016; Vila-Cha et al. 2012). Because the progressive decrease in discharge rates is typically paralleled by an increase in surface EMG amplitude, it has been generally assumed that the contraction can be sustained by the recruitment of additional motor units, which is supported by experimental observations (Adam and De Luca 2005; Carpentier et al. 2001). On the other hand, other studies have challenged the observation of a continuous decrease in discharge rate during submaximal fatiguing contractions (Adam and De Luca 2005; Dorfman et al. 1990; Garland et al. 1997; Griffin et al. 2000; Kuchinad et al. 2004; Mettler and Griffin 2016). In these studies, an increase in motor unit discharge rates was observed after an initial decrease, and this behaviour was linked with a decrease in whole-muscle single-twitch force (Adam and De Luca 2005). These results implied that neural

adjustments might be required to compensate for changes in contractile properties in order to maintain a steady force. This diverse motor unit behaviour across studies may be related to the wide variety of protocols utilized to assess fatigue (Enoka and Duchateau 2008; Hunter et al. 2004), the specific muscle under study and the force level assessed. Regardless of the protocol employed and the target muscle assessed, it has been difficult to track the same motor units during the entire duration of fatiguing contractions using intramuscular EMG recordings, and this difficulty has generated controversy on the actual adaptations in motor unit behaviour with fatigue (Enoka 2019). Identifying the activity of the same motor units during both fatiguing and non-fatiguing contractions is essential to unravel the neural control of fatigue, but, it is extremely challenging due to the different levels of superimposition of motor unit action potentials in the recorded signals. Moreover, the waveforms of the motor unit action potentials (MUAPs) change during the course of different contractions, specifically during contractions until failure, and therefore to track the MUAPs of the same motor units in these recording conditions is not always possible. In this study, we aimed to investigate the changes in motor unit discharge rate and contractile properties of two synergistic muscles by tracking a representative number of motor units during a sustained submaximal isometric contraction until task failure. For this purpose, we developed a novel approach of time-domain motor unit tracking that assures high accuracy in the observed motor unit properties with fatigue. We coupled this tracking approach with a recently developed technique to estimate the characteristics of (fused) motor unit twitches quantified during the course of the sustained contraction (Negro and Orizio 2017). Finally, we compared the firing properties of the same motor units identified at task failure and a higher-force non-fatiguing contraction in order to assess the neural mechanisms responsible for task failure. The results provide a comprehensive characterisation of the neural and contractile adjustments of motor units with fatigue and prove the inability of the central nervous system to sufficiently increase the neural drive to muscle with fatigue.

METHODS

Participants

Sixteen healthy and physically active men [mean (SD) age: 28 (4) yr, height: 177 (5) cm, mass: 78 (6) kg] without a history of neuromuscular disorders or previous lower limb surgery, were recruited. Participants were asked to avoid any strenuous physical activity 24 h before the measurements. The Ethics Committee of the Universität Potsdam approved the study (approval no. 26/2015), in accordance with the Declaration of Helsinki (2004). All participants gave written, informed consent.

Experimental Protocol

The participants performed submaximal and maximal knee extension (dominant leg) contractions on an isokinetic dynamometer (CON-TREX MJ; PHYSIOMED, Regensdorf, Switzerland). All isometric contractions were exerted with the knee flexed to 90° and hip flexed to 80° (chair was reclined by 10°). The participant's torso, waist and contralateral leg were strapped to the chair in order to prevent compensatory movements throughout the trial. After placement of the surface EMG electrodes (see Data Acquisition), subjects performed three maximal voluntary contractions (MVC) of knee extension for 5 s and each of these trials was separated by 2 min of rest. The highest MVC value was used as a reference to define the submaximal torque level. After 5 min of rest, and following a few familiarization trials, subjects performed a submaximal isometric knee extension contraction at 50% MVC by following a target that had a trapezoidal waveform presented in a computer screen (5 s ramp-up and ramp-down contraction with a 15 s hold-phase). Then, after 15 min of rest, the participants performed a contraction at 30% MVC until exhaustion. This contraction level was selected as participants typically reach knee-extension task failure after a few minutes (Martinez-Valdes et al. 2017a; Vila-Cha et al. 2012) and the intensity is well below the force level corresponding to full motor unit recruitment in both investigated muscles (Enoka and Fuglevand 2001). In each of these trials, the participants also received visual

feedback of the torque applied by the leg to the dynamometer. Time to task failure was defined as the time instant when the subject exerted a force 10% MVC below the target force for a 2 s interval of time (Castronovo et al. 2015). Another MVC was performed at the end of the sustained contraction to verify the presence of fatigue.

Data Acquisition

Surface EMG signals were recorded from the vastus medialis (VM) and vastus lateralis (VL) in monopolar derivation with 2-dimensional adhesive grids (Spes Medica, Salerno, Italy) of 13 (rows) x 5 (columns) equally spaced electrodes (1-mm diameter, interelectrode distance of 8 mm). EMG signals were initially recorded during a brief voluntary contraction during which a linear dry electrode array of 8 silver-bar electrodes (1-mm diameter, 5-mm length, 5-mm interelectrode distance; SA 8/5; OT Bioelettronica, Torino, Italy) was moved over the skin to detect the location of the innervation zone and fibre alignment (Martinez-Valdes et al. 2016). After the skin was shaved and cleansed with abrasive paste and water, the electrode cavities of the grids were filled with conductive paste (Spes Medica). High-density surface EMG (HDsEMG) grids were positioned between the proximal and distal tendons of the VM and VL muscles with the electrode columns oriented along the muscle fibers as previously described (Martinez-Valdes et al. 2018a; Martinez-Valdes et al. 2018b). Reference electrodes were positioned over the malleoli and patella of the dominant leg. EMG and torque signals were sampled at 2048 Hz and converted to digital data by a 12-bit analog-to-digital converter (3 dB, bandwidth 10–500 Hz, 256-channel EMG amplifier; EMG-USB 2; OT Bioelettronica). EMG signals were amplified by a factor of 500 for the 50% MVC contractions and a factor of 1000 for the sustained 30% MVC contractions. Data were analyzed offline using MATLAB 2017b (The Math-Works, Natick, MA). The 64-monopolar EMG channels were re-referenced offline to form 59 bipolar channels as the differences between adjacent electrodes in the muscle fibres direction.

Signal Analysis: motor unit decomposition and tracking

The EMG signals recorded during the submaximal contractions were decomposed offline with a method that has been extensively validated (Negro et al. 2016). Since EMG amplitude increases and MUAP morphology changes throughout the time-course of a sustained submaximal fatiguing contraction (Beck et al. 2005), it is not possible to apply the decomposition algorithm for the full duration of the contraction. The algorithm indeed relies on the stationarity of the action potential waveforms, something that is not satisfied in fatiguing contractions. Therefore, for the 30% MVC contraction, the HDsEMG signals were divided into 30 s intervals, with an overlap of 15 s between intervals. Each interval was then decomposed individually and the accuracy of the decomposition was tested with the silhouette (SIL) measure for each motor unit. SIL is the difference between the within and between-cluster sums of point-to-centroid distances, normalized dividing by the maximum of the two values. SIL is a normalized accuracy index for EMG decomposition that can be directly associated to the accuracy of the decomposition (Negro et al. 2016). Only motor units with a SIL greater than 0.90 were considered for further analysis (Martinez-Valdes et al. 2017a; Negro et al. 2016). Then, the decomposition accuracy was improved by manual editing of consecutive discharges separated from each other by <33.3 ms or >200 ms and the iterative estimation of the motor unit extraction filters. This semi-automatic approach was used to iteratively improve the accuracy of the automatic decomposition algorithm by the visual interaction with an expert operator (Boccia et al. 2019; Martinez-Valdes et al. 2020). Following the decomposition, the motor units were tracked across the decomposition intervals by direct cross-correlation of the discharge times (time domain analysis) identified during the overlapping time portions of the 30 s processing intervals. In these overlapped portions, discharges were considered to belong to the same motor unit when at least 70% of the discharge times were identified by the two independent decompositions in the two 30 s intervals within a delay of 5 ms (**Figure 1**). In this way, the tracking of the motor units did not depend on the shape of the action potential waveforms, which varied over time.

Moreover, since the decomposition of the 30 s intervals were all performed independently, the identification of the same discharge pattern for the identified sources (motor units) can only be associated to the detection of the same motor units. With this approach, motor units could be tracked over time with the only assumption that their action potential waveforms were stable within each of the 30 s intervals.

The modulation in discharge rates for each of the tracked motor units was filtered and smoothed (400 ms Hanning window) and then correlated to the torque signal to compare common fluctuations in torque and discharge rate. Since EMG signals during sustained submaximal fatiguing contractions become highly interferential, we verified that the fluctuations in firing rate were highly correlated to the torque signal (see Results) to further support the accuracy of the decomposition (Enoka 2019; Negro et al. 2009; Thompson et al. 2018). Any decrease in this correlation may be due to the erroneous identification of the discharge times (Enoka 2019; Nawab et al. 2008).

As an additional validation step, the two-dimensional representation of the MUAPs (Martinez-Valdes et al. 2017b), was extracted by spike-triggered averaging from the first and last 50 firings of each motor unit (beginning and end of the contraction). Changes in MUAP shape are expected during the time-course of a fatiguing contraction (i.e. MUAP size and duration), due to adjustments in peripheral properties (e.g., conduction velocity) (Beck et al. 2005). This was the reason for developing the tracking method which is not based on MUAP waveforms. Yet, based on previous studies (Carpentier et al. 2001; Garland et al. 1997), it was expected that the changes in MUAP shapes would be progressive and that they would not completely disrupt the initial spatial representations of MUAPs. Therefore, it was assumed that the MUAP waveforms estimated at the beginning and end of the contraction would not be completely uncorrelated. Based on this assumption, only motor units with MUAP waveforms which were correlated by > 0.8 at the end with respect to the beginning of the contraction were considered for

194 further analysis (Boccia et al. 2019). This indirect criterion for decomposition accuracy is based on the
195 observation that discharge times were identified by independent decompositions of the 30 s intervals
196 and, therefore, it would be highly unlikely that spike-triggered averaging on these estimated discharges
197 would lead to similar MUAP waveforms if the decomposition was incorrect. Moreover, since the
198 procedure for tracking over time did not involve the MUAP waveforms, this validation measure was
199 independent from the tracking criterion. An example of this procedure for one motor unit from the VM
200 can be seen in **Figure 2**.

201 Finally, and in order to check the effects of fatigue on discharge rate at task failure, motor units were
202 matched between contractions at 50% MVC and the end of 30% MVC to study the behaviour of later
203 recruited motor units just before task failure (cross correlation level of 2D MUAP waveforms >0.8)
204 (Martinez-Valdes et al. 2017b). In addition, we matched motor units from the contractions at 50% MVC
205 with the beginning and end of the 30% MVC contractions (2D MUAP cross-correlation >0.8), in order to
206 compare the level of discharge rate between motor units identified at 50% MVC and earlier recruited
207 units at 30% MVC during task failure (Martinez-Valdes et al. 2017b).

208 Motor unit and torque signal analysis

209 Mean discharge rate, the coefficient of variation for the interspike interval (CoVisi) and the coefficient of
210 variation of torque (CoV torque) from early recruited motor units (motor units that were recruited at
211 the beginning of the contraction), were calculated from the stable torque region of the sustained
212 contraction until task failure in 1 s epochs. The motor unit recruitment threshold was defined as the
213 knee extension torque (%MVC) at the time when the motor unit began discharging action potentials.

214 The values from the 1 s epochs were then averaged over time-normalized intervals with a duration of 10%
215 of the time to task failure (i.e., 10-100% of time to task failure in increments of 10%). Cross-correlation
216 between low-frequency (<5 Hz) fluctuations in motor unit dicharges and torque was also computed for

each of the 10 segments. This comparison was made between single motor units and torque (each spike train was correlated individually to the torque signal) to decrease the chance of high cross-correlation values due to the averaging of larger populations of motor units (Negro et al. 2009; Thompson et al. 2018).

For statistical reasons, the discharge behaviour and the properties of MUAPs were analysed only for the motor units active for the entire duration of the contraction. The discharge rates of motor units that were identified after the beginning of the contraction were analysed separately. Since both the early and later recruited motor units showed a time point after which discharge rates increased following the initial decrease (see Results), this time point was compared across all identified motor units (see Statistics).

Interference EMG

The root mean square amplitude (RMS) obtained from the sustained submaximal contractions was averaged over all channels of the electrode grid for each muscle (59 bipolar channels). As with motor unit variables, the RMS was computed from the HDsEMG signals in intervals of 1 s and also normalized in 10 segments as defined above. Differences in RMS amplitude were also compared between the non-fatiguing 50% MVC contraction and the last epoch before task failure (30% MVC, epoch 10). For 50% MVC, RMS values were determined from the steady-torque part of the contraction (average RMS value of ten 1 s windows).

Motor unit contractile properties

Motor unit twitch torque during the course of the contraction (fused twitches) was determined by a recently proposed technique based on the deconvolution of the torque signal using identified discharge times of a population of motor units (Negro and Orizio 2017). In this study, a simplified model of twitch

profile characterized only by two parameters (peak amplitude and time to peak) was used (Fuglevand et al. 1993). Briefly, a large range of peak amplitude and time to peak values were explored. The reconstruction of the force profile was performed using motor unit firing data and twitch waveforms. A band-pass filter (0.75-10 Hz) was applied to both reconstructured and original force profiles for each twitch parameter combination in order to limit the influence of unidentified motor units. The squared Euclidean distance was used as a measure of similarity between the two signals (original and reconstructed force) and the twitch parameters providing minimum distance were used as the final estimation. Since both approaches may result in multiple minima, we used the area of the estimated twitch profile as a measure of contractile properties. To obtain accurate estimates, this analysis requires a large number of motor units (>10) identified over long time intervals (>20s) (Negro and Orizio, 2017), therefore it was applied only to the VM, for which a larger number of motor units was usually identified compared to VL (see Results), and for longer epochs (20, 40, 60, 80 and 100% of total endurance time) than those used for the other analyses. Despite these choices, the assumptions for this analysis were met only by the data from 4 participants [mean (SD) age: 27 (6) yr, height: 178 (5) cm, mass: 77 (5) kg]. The average motor unit twitch force was estimated from these participants only and characterised by its area.

Statistical Analysis

All results are expressed as mean and standard deviation (SD). All variables were tested for normality using the Shapiro–Wilk test and statistical significance was set at $p < 0.05$. MVCs performed at the beginning and end of the sustained contractions were compared by t-tests. Piecewise regressions and polynomial models (2^{nd} order) were used to fit the variables extracted for motor units (early recruited) and torque variability. The model leading to the highest correlation coefficient with the original data was used to fit the data (Loscher et al. 1996b). The piecewise regression analyses showed two distinct

phases of the contraction for all variables analysed (see Results). Thus, the intersection point of the two regression lines [piecewise regression (Beaver et al. 1985)] was defined as the reversal time instant (i.e., transition from a positive/null to a negative/null slope or viceversa). The time instants (seconds) of reversal for discharge rate, CoVisi and CoV for torque were analysed by two-way repeated mesures ANOVA with factors the variable (discharge rate, CoVisi, CoV torque) and muscle (VM and VL). Since from this analysis, the reversal points were not different between variables or muscles (see Results), we averaged the reversal time instants across muscles and variables. This averaged value will be referred in the following to as motor unit behaviour reversal point as it defines the time instants where central motor unit properties (i.e. discharge rate, recruitment and CoVisi) and contractile (peripheral motor unit properties) variables investigated, changed their behaviour. For this reason, the motor unit behaviour reversal point separates the contraction in two phases, which are characterized by different adaptations. The association between the motor unit behaviour reversal point and the total endurance time was analysed by linear correlation. Piecewise linear regressions were used to fit the discharge rate data from later recruited motor units (i.e., motor units not active from the beginning of the task) and the break point between the two lines was considered the reversal time instant for these motor units and analysed by two way repeated measures ANOVA to compare it with the reversal time for early recruited units (factors: later/early recruited units; and muscle VM/VL). The number of later recruited units that were activated before and after the motor unit behaviour reversal point (phase 1 vs phase 2) was also compared by two-way repeated measures ANOVA (factors: phase 1/phase 2 and muscle VM/VL). Two-way repeated measures ANOVA (factors of time: 10 epochs and muscle: VM and VL) was used to compare each of the normalized variables, which consisted of 10 segments of RMS amplitude, discharge rate, CoV isi, single-motor unit/torque cross-correlation and CoV of torque. The firing behaviour of the common units identified at 50% MVC and 30% MVC preceding task failure (for both early and later recruited units) was compared by three-way repeated measures ANOVA with factors muscle (VM and

VL), force (50% and 30% MVC) and recruitment (early vs late). Finally, RMS amplitude between 50% MVC and 30% MVC immediately before task failure was compared by two-way repeated measures ANOVA (factors: muscle and force level). Bonferroni corrected t-tests were performed when ANOVA was significant.

RESULTS

Endurance time and maximal torque generation capacity

Participants sustained the 30% MVC knee extension contraction for 122.8 (33.3) s and MVC peak torque significantly decreased by 18.1 (7.5)% immediately following the contraction (from 198.0 (28.7) Nm to 162.1 (25.6) Nm, $p<0.001$).

Motor unit identification and tracking during sustained contraction until failure (30% MVC)

Motor units could not be tracked in two of the 16 subjects due to poor signal quality and therefore the results are presented for 14 participants [mean (SD) age: 29 (2) yr, height: 177 (6) cm, mass: 78 (7) kg]. An average of 5 (3) and 4 (3) motor units could be tracked for the entire contraction duration per subject for VM and VL, respectively. The MUAP waveforms of these motor units were similar at the beginning and end of the contraction (cross-correlation coefficient of 0.81 (0.07) and 0.80 (0.04) for VM and VL, respectively). The average recruitment threshold of these units was 22.6 (4) and 21.7 (6.3) % MVC for VM and VL respectively ($p=0.22$). Finally, an average of 4 (2) and 3 (3) motor units per subject (values were rounded to the closest integer) were recruited later and were followed until the end of the contraction for the VM and VL, respectively. The number of later recruited units was significantly larger during the second phase of the contraction (after the motor unit behaviour reversal point; see next section) as on average, we could identifiy the recruitment of 1 (1) motor unit in phase one and 2 (2) motor units in phase two (per participant), in both muscles (phase effect: $p<0.0001$, $\eta 2=0.64$).

Motor Unit Behaviour

The representative behavior of VM motor units from one participant can be seen in **Figure 3**. In this participant, 10 motor units could be followed from the beginning of the contraction and a total number of 16 motor units were identified throughout the entire course of the contraction. In this example, early recruited units showed an initial decrease in discharge rate until approximately 50% of endurance time, and then increased their discharge frequency until the end of the contraction. Later recruited motor units followed the same behavior of early recruited units, with their discharge rates increasing after 50% of the endurance time, irrespective of the time of recruitment. Motor units that were recruited after 50% of the endurance time increased their discharge rates during the entire duration of their activation. All motor units showed a discharge rate at the end of the contraction that was similar or slightly higher than the discharge rate at the beginning of their activation. This representative behaviour was consistent for the group of participants. At the group level, the time instant of reversal in discharge rate was not different between early and later (recruited before and after the deflection point) recruited motor units, nor between muscles (VM early: 66.7 (18.2) s vs. VM later: 65.3 (20) s, VL early: 66.4 (21.8) s vs. VL later: 65.8 (21) s, $p>0.78$ for main effects). The 2^{nd} order polynomials explained 61.1 (16.3)% and 63.4 (18.1)% of the variance in discharge rate during the sustained contractions for VM and VL, respectively **(Figure 4)**. Only one subject showed a continuous decrease in firing rates (bright-green dots in **Figure 4**). Across all participants, the mean discharge rates decreased significantly until approximately 40% of the normalized endurance time ($p=0.039$, 95% CI of difference between 10% and 40% endurance time: 0.02 to 2.1 Hz) and subsequently increased until task failure, where discharge rates were significantly higher than those at the beginning of the contraction ($p<0.001$, 95% CI difference: -2.5 to -0.5 Hz) (**Figure 5A**). There was no difference in mean firing rates between muscles (interaction: muscle x time, $p=0.27$, $\eta^2=0.09$). This increase in discharge rate from ~40% of endurance time was also concurrent with a significant increase in discharge rate variability (CoVisi, time effect: $p<0.0001$, $\eta^2=0.55$) (**Figure 5B**)

and CoV torque (time effect: $p<0.0001$, $\eta^2=0.55$) (**Figure 5C**), which were both constant over time before this time instant. Additionally, the correlation between torque and firing rate fluctuations of single motor units also increased after 40% of endurance time (time effect: $p<0.0001$, $\eta^2=0.35$) (**Figure 5D**).

Associations between motor unit discharge rate and endurance time

The association between the reversal time points in discharge rate and CoVisi in VM and VL motor units and CoV torque can be seen for a representative participant in **Figure 6.** These variables changed their trends at similar instants in time. On a group level, the reversal points were not significiantly different among the variables analysed and between muscles (for discharge rate, CoV force and CoVisi: 66.8 (24.9) s, 66.5 (23) s and 64.4 (25.3) s for VM, and 64.6 (23.1), 65.9 (22.6) and 68.9 (29) s for VL; P=0.945). Thus, any of these instants represented the change in central (i.e. discharge rate) and peripheral (i.e. twitch area) motor unit behaviour during the course of the fatiguing contraction. For this reason, we averaged these time instants and obtained the motor unit behaviour reversal point. The motor unit behaviour reversal point accurately predicted total endurance time ($r=0.93$, $R^2=0.87$, $p<0.0001$, **Figure 7**).

Comparison of motor unit discharge rate between non-fatiguing 50% MVC contractions and 30% MVC contractions at task failure

The discharge rate for both earlier and later recruited units during 30% MVC during the last seconds before task failure (last epoch) was lower than the average discharge rate of the same motor units when activated at 50% MVC. The representative behaviour of a VL motor unit that was tracked between 50% MVC and 30% MVC just before task failure can be seen in **figure 8**. A total of 3 (2) and 2 (2) motor units could be matched per subject between 50% MVC and 30% MVC few seconds before task failure (late recruited units) for VM and VL, respectively [average cross correlation coefficient of 0.87 (0.06) and 0.86 (0.05)] . Additionally, 2 (1) and 2 (1) motor units per subject could be matched between 50% MVC and the beginning and end of the 30% MVC contraction (behaviour of earlier recruited at task failure) for VM

and VL, respectively [average cross-correlation coefficient of 0.9 (0.03) and 0.83 (0.02)]. As expected, earlier recruited units had a higher discharge rate (at both 50% MVC and 30% MVC) compared to later recruited units (recruitment effect: $p=0.005$, $\eta 2=0.46$), **figure 9**. However, both ealier and later recruited units always had a firing frequency significantly higher at 50% MVC (force effect: $p<0.0001$, $\eta 2=0.79$), **figure 9**.

Interference EMG

RMS amplitude increased linearly throughout the sustained contraction (time effect: $p<0.0001$, $\eta 2=0.74$) in both muscles (**Figure 10a**). There was a significant interaction between VM and VL, as VM showed a greater increase in RMS amplitude throughout the course of the contraction (interaction: muscle x time, $p<0.0001$, $\eta 2=0.65$). RMS amplitude was similar between the 50% MVC contraction and the 30% MVC contraction at failure in both muscles (force effect: $p=0.44$, $\eta 2=0.05$, **figure 10b**).

Assessment of contractile properties

Twitch area and its relationship with discharge rate for one participant can be observed in **Figure 11**. For this participant, the twitch area increased over time until approximately 40% of the endurance time and then decreased, reaching its minimum value at 100% of total endurance time. Even though we could not directly compare statistically the reversal points in neural properties and twitch force (as the twitch had to be estimated in a different time interval), we could observe that the point where neural adjustments reversed their behaviour approximately coincided with the point of maximum twitch force (blue line). This behavior was also observed in the other three participants for which the average twitch could be estimated. Overall, twitch area declined in this group of subjects by 35.3% (range from 0% to 61.8%) at failure compared to baseline (20% of endurance time).

DISCUSSION

Using a new time-domain technique of motor unit tracking during sustained submaximal fatiguing contractions we were able to follow the firing behavior of a representative number of units until task failure and compare them with the same motor units identified during a higher-force non-fatiguing contraction. The results show two distinct phases in motor unit firing and contractile properties, characterized by different motor unit behaviour. In the first phase, motor unit discharge rates decreased, and interspike interval and force variabilities remained constant. At a well defined time instant, which marked the beginning of the second phase, these three variables began to increase until task failure. The time point marking the separation of the two phases predicted the time to failure. The contractile motor unit properties also changed differently in the two phases, with an increase in twitch area in the first phase and a decrease in the second phase. Finally, the later increase in discharge rate, peaked at a slower firing frequency compared to a non-fatiguing 50% MVC contraction, revealing possible saturation of the motor unit unit pool due to strong central inhibition or lack of additional excitation. Taken together, these results show that both motor unit central and peripheral processes during sustained submaximal contractions until failure, in the vasti muscles, do not progress similarly throughout the contraction but are rather characterized by at least two distinct stages. Since the beginning of the second phase determines the time of task failure, the adjustments needed in the second phase are presumably the limiting factor of the neuromuscular system in maintaining the task.

Trends of motor unit discharge rate over time

Although it is generally accepted that motor unit discharge rate decreases linearly during submaximal fatiguing contractions until failure (Enoka and Duchateau 2008), many of the studies analysing motor unit firing properties during these contractions have reported an initial decrease and later increase in firing frequency (Adam and De Luca 2005; Bigland-Ritchie et al. 1986; Castronovo et al. 2015; Dorfman et al. 1990; Garland et al. 1997; Griffin et al. 2000; Kuchinad et al. 2004; Mettler and Griffin 2016).

Although the divergence in motor unit behaviour could be likely related to differences in the tasks performed to study fatigue (Enoka and Duchateau 2008), it is important to note that all previous studies used decomposition methods based on MUAP template-matching to follow motor units throughout the contractions with a high probability of erroneous identification of discharges. In this study, we have proposed an approach that does not rely on tracking MUAP waveforms, which allowed us to successfully track a more representative number of motor units during the entire duration of a sustained contraction until failure. Moreover, using a recent deconvolution algorithm (Negro and Orizio 2017) we could monitor changes in motor unit twitch areas from a subset of participants during the course of the contraction. This particular method, can provide a more accurate assessment of motor unit twitch force compared to single-twitch whole-muscle force measurements (Adam and De Luca 2005) and spike-triggered averaging techniques (Carpentier et al. 2001). Therefore, utilizing these approaches, we identified a biphasic behaviour in the neuromuscular processes underlying fatigue and associated this behaviour with endurance time.

Besides methodological constraints, other factors such as contraction duration (sustained contraction for a fixed period of time vs sustained contraction until failure), force level and muscle studied, might be behind the differences in results across studies. For instance, all studies that have identified a non-linear firing response have performed submaximal contractions until task failure (Adam and De Luca 2005; Bigland-Ritchie et al. 1986; Castronovo et al. 2015; Dorfman et al. 1990; Garland et al. 1997; Griffin et al. 2000; Kuchinad et al. 2004; Mettler and Griffin 2016), while those reporting monotonic decreases in discharge rate have been performed for either a fixed duration (Mottram et al. 2005; Pascoe et al. 2014; Riley et al. 2008) or until failure (Carpentier et al. 2001; Dalton et al. 2010; Garland et al. 1994; McManus et al. 2016). In the specific case of the studies from Carpentier et al. and Garland et al., the authors showed that motor unit behaviour could be related to the recruitment-threshold. In those studies, motor units with lower recruitment thresholds showed a linear decrease in discharge rate while

higher threshold units showed maintained or increased firing frequency. Considering that the average recruitment threshold of motor units that could be tracked for most of the sustained contraction was relatively high in the present study (22% MVC), the results are to be compared with those on the higher-threshold motor units of these previous studies. The next factor explaining the divergence in results across studies could be related to the exerted force level. Most of the studies reporting non-linear changes in discharge rate have used relatively low-force contractions, ranging from 20-30%MVC, while the studies reporting monotonic decreases have usually employed higher-force contractions, at 50% MVC (Carpentier et al. 2001; Enoka et al. 1989), from 10 to 64%MVC (Garland et al. 1994) or even 75% MVC (Dalton et al. 2010). The behaviour observed in the present study is likely specific for contractions at low to moderate forces. At very high forces, the rapid increase in excitation to the motor neuron pool may occur very early in the contraction and just induce a linear decrease in firing frequency, as commonly observed during maximal voluntary contractions (Bigland-Ritchie et al. 1983). Changes in discharge rate can also be muscle-specific. For instance, Adam and De Luca observed the same behaviour as reported in the present study for vastus lateralis (Adam and De Luca 2005) at 30%MVC, while monotonic reductions in discharge rate have been consistently reported for the first dorsal interosseous muscle (Carpentier et al. 2001; Enoka et al. 1989; McManus et al. 2016), regardless of the force level (30 or 50% MVC). These observations suggest that motor unit adjustments to fatigue may depend on muscle-specific properties, such as the upper limit of recruitment, and therefore the findings obtained from individual muscles cannot be generalized. Finally, it is also important to mention that most of previous studies relied on pooled firing rate data which considers each motor unit as an independent observation (even when belonging to the same subject). This can provide equivocal estimates of motor unit behaviour (Adam and De Luca 2005; Tenan et al. 2014) and therefore it is important to assess motor unit firing responses on a subject by subject basis, as done in the present study.

448 *Changes in contractile properties*

449 Our results showed that an increase in discharge rate is needed to compensate for the decline in the
450 total area of the motor unit twitch force **(Fig. 11)**. Early increases in twitch area (and concomitant
451 decreases in discharge rate) can be explained by post-activation potentiation (Fowles and Green 2003)
452 and twitch contraction time elongation, while later decreases in twitch area might be due to greater
453 accumulation of metabolic by-products, such as potassium, hydrogen ion, inorganic phosphate and
454 reactive oxygen and nitrogen species, among others affecting muscle fibre-contractile capacity and thus
455 twitch amplitude (McKenna et al. 2008). Consequently, changes in central mechanisms (motor unit
456 discharge rate and recruitment) should compensate for a decline in contractile properties in order to
457 maintain torque output, as shown in the present study.

458 *Common Synaptic input and changes in motoneuron excitability*

459 In 15 out of 16 subjects, all motor units followed the same biphasic behaviour **(Figure 3)**, likely reflecting
460 the strong common synaptic input received by the motor unit pool as the contraction progressed
461 (Castronovo et al. 2015). This increase in common input is also typically accompanied by higher torque
462 and discharge rate variability, and by stronger correlations between fluctuations in muscle force and
463 discharge rate (Castronovo et al. 2018; Castronovo et al. 2015). Consistent with these observations, our
464 data shows that CoV of torque and CoVisi, and the correlation between fluctuations in motor unit
465 discharge rates and torque, increased from 40% of the endurance time until task failure **(Figure 5)**.
466 Moreover, a greater number of motor units were recruited during the second phase of the contraction,
467 in agreement with an increase in drive to motoneurons. This mechanism is possibly required to
468 compensate for the gradual decrease in twitch area and the increased inhibition experienced by the
469 motoneuron pool during this phase of the contraction. Motoneuron inhibition may occur due to a
470 number of mechanisms, including decreased muscle spindle activity (Brunetti et al. 2003), increased

firing of type III and IV afferents (Martinez-Valdes et al. 2020), and decreased recurrent inhibition (Taylor et al. 2016). However, these inhibitory inputs could be compensated by increasing supraspinal excitatory voluntary drive, as previously shown in studies assessing corticospinal excitability during sustained submaximal contractions until failure (Levenez et al. 2008; Sacco et al. 1997; Taylor et al. 1996). Thus, the increased discharge rate observed in the second phase might be due to an increased supraspinal input into the motoneuron pool. Nevertheless and like motor unit recordings, not all studies have reported an increase in corticospinal excitability during fatigue, which may be related to differences in protocols to measure motoneuron excitability, in particular contraction duration (contractions sustained for a fixed period of time vs contractions until failure). Most studies informing an increase in corticospinal excitability have employed sustained submaximal contractions until failure (Levenez et al. 2008; Sacco et al. 1997), while those repoting decreases have usually employed sustained (or intermittent) contractions for a fixed duration (i.e. (Finn et al. 2018; McNeil et al. 2011; Sogaard et al. 2006), which did not reach full exhaustion. Therefore, future studies should aim to combine motor unit recordings with measures of spinal and cortico-spinal excitability during sustained contractions until failure, in order to understand the relationship between the biphasic motor unit firing behaviour observed in the present study and motoneuron excitability.

Motor unit saturation at task failure

Despite the increase in discharge rates in the second stage, these firings did not reach values attainable at greater forces in absence of fatigue **(Figures 8 and 9)**. This finding provides unique evidence to further support a primary role of central rather than peripheral mechanisms for task failure, as the 40-50% decline in twitch force observed by the end of the contraction could have been still compensated by increasing discharge rates. Consistent with these findings, previous studies have shown that EMG activity just before task failure is lower than that observed during an MVC, even when subject's exert

maximal effort (Fuglevand et al. 1993). Our findings confirm these observations, as RMS only reached the level of a 50% MVC contraction **(Figure 10B)**. Although EMG combines information on both central and peripheral factors, these findings can be interpreted as an inability to drive the muscle further at the point of failure (Loscher et al. 1996a). It is evident that even when participants exert maximal effort, this increase in firing frequency (and probably motor unit recruitment) would not be sufficient to maintain the task. The descending drive generated by maximal efforts could be opposed by an increase in inhibition to motoneurons or higher centers, or reductions in motoneuron excitability. Previous studies (Kennedy et al. 2014; 2013) found evidence for increased inhibition of central drive via fatigue-induced activation of high threshold afferents. An additional possibility is a decrease in intrinsic excitability of motoneurons. During prolonged activation, motoneurons exhibit spike frequency adaptation (Kernell and Monster 1982; Sawczuk et al. 1995), although this mechanism does not induce the severe saturation seen in the present study. The intrinisic excitability of motoneurons is in fact primarily controlled by neuromodulatory inputs that originate in the brainstem and act via axons releasing the monoamines serotonin and norepinephrine. A seminal study by Fornal et al. (Fornal et al. 2006) showed that, as cats ran to exhaustion on a treadmill, firing rates in serotonergic neurons in the caudal raphe nuclei initially increased but then began to fall. The caudal raphe is the primary source of serotoninergic axons that project to motoneurons and the actions of this serotonergic projection on motoneuron excitability are profound, increasing the efficacy of synaptic inputs as much as 3-5 fold (Heckman and Enoka 2012; Heckmann et al. 2005). Consequently a decrease in this neuromodulatory drive could greatly decrease the efficacy of descending motor commands. While this speculation is reasonable, the work in the cat was carried out for long periods of locomotion, a different motor task than in the present study. In the case of sustained submaximal contractions in humans, a recent study has shown that increased availability of serotonin influences central fatigue, particularly increasing perceptions of fatigue and shortening the silent period (Thorstensen et al. 2020). These adaptations did not influence

motor pathways nor motor performance, and therefore the authors concluded that serotonergic neurotransmission influence supraspinal processes without altering motor pathways during low-force sustained muscle contractions. Nevertheless, it is important to mention that the authors did not perform a contraction until task failure. Therefore, it could be possible that serotonin decreases the excitability of spinal motoneurons during submaximal contractions at task failure in a similar extent to what has been reported during maximal fatiguing contractions (Kavanagh et al. 2019). However, this needs to be confirmed in future investigations. Taken together, we can suggest that a combination of increased inhibition and decreased intrinsic excitability of motoneurons seems a plausible mechanism for firing rate saturation in the fatigue task performed in this study.

Limitations

One limitation of this study is that the results on contractile properties could only be obtained from four participants, because of constraints of the analysis method used to estimate twitch force. Additionally, the results have been obtained for only one submaximal force level (30% MVC). A previous study (without motor unit tracking) reported similar increases in CoV force, CoVisi and RMS amplitude between the beginning and end of submaximal contractions at 20 and 50% MVC, but not at 75% MVC (Castronovo et al. 2015). Therefore, it is important to confirm the observed behaviour at different force levels. Task-dependent effects of fatigue, need to be also studied in order to assess whether the same mechanisms observed in the current study can be transferred to other tasks. Finally, the analysis of the rate of motor unit recruitment during the contraction is limited by the small proportion of motor units identified with respect to the total number of active motor units. Future methods combining HDsEMG and thin-film multi-channel intramuscular electrodes (Muceli et al. 2015) could aid to sample larger populations of motor units and directly determine the number of units active during submaximal sustained contractions until failure.

Conclusion

During sustained submaximal knee-extension contractions until failure, the behaviour of motor units is characterized by two distinct phases. The time of transition from the first to the second phase marks the beginning of an increase in excitatory drive to motor neurons and is a predictor of task failure. Despite of the increase in excitatory drive during the second phase, the contraction cannot be sustained possibly due to progressive motor neuron inhibition or reduced level of excitation as the later increase in firing rate saturates at a much slower discharge rate compared to the one recorded at a higher-force non-fatiguing contraction. This finding provides strong evidence suggesting that central rather than peripheral mechanisms are the main determinants for task failure.

REFERENCES

Adam A, and De Luca CJ. Firing rates of motor units in human vastus lateralis muscle during fatiguing isometric contractions. *J Appl Physiol (1985)* 99: 268-280, 2005.

Beaver WL, Wasserman K, and Whipp BJ. Improved detection of lactate threshold during exercise using a log-log transformation. *J Appl Physiol (1985)* 59: 1936-1940, 1985.

Beck RB, O'Malley MJ, Stegeman DF, Houtman CJ, Connolly S, and Zwarts MJ. Tracking motor unit action potentials in the tibialis anterior during fatigue. *Muscle Nerve* 32: 506-514, 2005.

Bigland-Ritchie B, Cafarelli E, and Vollestad NK. Fatigue of submaximal static contractions. *Acta Physiol Scand Suppl* 556: 137-148, 1986.

Bigland-Ritchie B, Johansson R, Lippold OC, Smith S, and Woods JJ. Changes in motoneurone firing rates during sustained maximal voluntary contractions. *J Physiol* 340: 335-346, 1983.

Boccia G, Martinez-Valdes E, Negro F, Rainoldi A, and Falla D. Motor unit discharge rate and the estimated synaptic input to the vasti muscles is higher in open compared with closed kinetic chain exercise. *J Appl Physiol (1985)* 127: 950-958, 2019.

Brunetti O, Della Torre G, Lucchi ML, Chiocchetti R, Bortolami R, and Pettorossi VE. Inhibition of muscle spindle afferent activity during masseter muscle fatigue in the rat. *Exp Brain Res* 152: 251-262, 2003.

Carpentier A, Duchateau J, and Hainaut K. Motor unit behaviour and contractile changes during fatigue in the human first dorsal interosseus. *J Physiol* 534: 903-912, 2001.

Castronovo AM, Mrachacz-Kersting N, Stevenson AJT, Holobar A, Enoka RM, and Farina D. Decrease in force steadiness with aging is associated with increased power of the common but not independent input to motor neurons. *J Neurophysiol* 120: 1616-1624, 2018.

Castronovo AM, Negro F, Conforto S, and Farina D. The proportion of common synaptic input to motor neurons increases with an increase in net excitatory input. *J Appl Physiol (1985)* 119: 1337-1346, 2015.

Dalton BH, Harwood B, Davidson AW, and Rice CL. Recovery of motoneuron output is delayed in old men following high-intensity fatigue. *J Neurophysiol* 103: 977-985, 2010.

Dorfman LJ, Howard JE, and McGill KC. Triphasic behavioral response of motor units to submaximal fatiguing exercise. *Muscle Nerve* 13: 621-628, 1990.

Enoka RM. Physiological validation of the decomposition of surface EMG signals. *J Electromyogr Kinesiol* 46: 70-83, 2019.
Enoka RM, and Duchateau J. Muscle fatigue: what, why and how it influences muscle function. *J Physiol* 586: 11-23, 2008.
Enoka RM, and Fuglevand AJ. Motor unit physiology: Some unresolved issues. *Muscle & Nerve* 24: 4-17, 2001.
Enoka RM, Robinson GA, and Kossev AR. Task and fatigue effects on low-threshold motor units in human hand muscle. *J Neurophysiol* 62: 1344-1359, 1989.
Finn HT, Rouffet DM, Kennedy DS, Green S, and Taylor JL. Motoneuron excitability of the quadriceps decreases during a fatiguing submaximal isometric contraction. *J Appl Physiol (1985)* 124: 970-979, 2018.
Fornal CA, Martin-Cora FJ, and Jacobs BL. "Fatigue" of medullary but not mesencephalic raphe serotonergic neurons during locomotion in cats. *Brain Res* 1072: 55-61, 2006.
Fowles JR, and Green HJ. Coexistence of potentiation and low-frequency fatigue during voluntary exercise in human skeletal muscle. *Can J Physiol Pharmacol* 81: 1092-1100, 2003.
Fuglevand AJ, Zackowski KM, Huey KA, and Enoka RM. Impairment of neuromuscular propagation during human fatiguing contractions at submaximal forces. *J Physiol* 460: 549-572, 1993.
Garland SJ, Enoka RM, Serrano LP, and Robinson GA. Behavior of motor units in human biceps brachii during a submaximal fatiguing contraction. *J Appl Physiol (1985)* 76: 2411-2419, 1994.
Garland SJ, Griffin L, and Ivanova T. Motor unit discharge rate is not associated with muscle relaxation time in sustained submaximal contractions in humans. *Neurosci Lett* 239: 25-28, 1997.
Griffin L, Ivanova T, and Garland SJ. Role of limb movement in the modulation of motor unit discharge rate during fatiguing contractions. *Exp Brain Res* 130: 392-400, 2000.
Heckman CJ, and Enoka RM. Motor unit. *Compr Physiol* 2: 2629-2682, 2012.
Heckmann CJ, Gorassini MA, and Bennett DJ. Persistent inward currents in motoneuron dendrites: implications for motor output. *Muscle Nerve* 31: 135-156, 2005.
Hunter SK, Duchateau J, and Enoka RM. Muscle fatigue and the mechanisms of task failure. *Exerc Sport Sci Rev* 32: 44-49, 2004.
Kavanagh JJ, McFarland AJ, and Taylor JL. Enhanced availability of serotonin increases activation of unfatigued muscle but exacerbates central fatigue during prolonged sustained contractions. *J Physiol* 597: 319-332, 2019.
Kennedy DS, McNeil CJ, Gandevia SC, and Taylor JL. Fatigue-related firing of distal muscle nociceptors reduces voluntary activation of proximal muscles of the same limb. *J Appl Physiol (1985)* 116: 385-394, 2014.
Kennedy DS, McNeil CJ, Gandevia SC, and Taylor JL. Firing of antagonist small-diameter muscle afferents reduces voluntary activation and torque of elbow flexors. *J Physiol* 591: 3591-3604, 2013.
Kernell D, and Monster AW. Time course and properties of late adaptation in spinal motoneurones of the cat. *Exp Brain Res* 46: 191-196, 1982.
Kuchinad RA, Ivanova TD, and Garland SJ. Modulation of motor unit discharge rate and H-reflex amplitude during submaximal fatigue of the human soleus muscle. *Exp Brain Res* 158: 345-355, 2004.
Levenez M, Garland SJ, Klass M, and Duchateau J. Cortical and spinal modulation of antagonist coactivation during a submaximal fatiguing contraction in humans. *J Neurophysiol* 99: 554-563, 2008.
Loscher WN, Cresswell AG, and Thorstensson A. Central fatigue during a long-lasting submaximal contraction of the triceps surae. *Exp Brain Res* 108: 305-314, 1996a.
Loscher WN, Cresswell AG, and Thorstensson A. Excitatory drive to the alpha-motoneuron pool during a fatiguing submaximal contraction in man. *J Physiol* 491 (Pt 1): 271-280, 1996b.
Martinez-Valdes E, Falla D, Negro F, Mayer F, and Farina D. Differential Motor Unit Changes after Endurance or High-Intensity Interval Training. *Med Sci Sports Exerc* 49: 1126-1136, 2017a.

Martinez-Valdes E, Farina D, Negro F, Del Vecchio A, and Falla D. Early Motor Unit Conduction Velocity Changes to High-Intensity Interval Training versus Continuous Training. *Med Sci Sports Exerc* 50: 2339-2350, 2018a.

Martinez-Valdes E, Guzman-Venegas RA, Silvestre RA, Macdonald JH, Falla D, Araneda OF, and Haichelis D. Electromyographic adjustments during continuous and intermittent incremental fatiguing cycling. *Scand J Med Sci Sports* 26: 1273-1282, 2016.

Martinez-Valdes E, Negro F, Falla D, De Nunzio AM, and Farina D. Surface electromyographic amplitude does not identify differences in neural drive to synergistic muscles. *J Appl Physiol (1985)* 124: 1071-1079, 2018b.

Martinez-Valdes E, Negro F, Farina D, and Falla D. Divergent response of low- versus high-threshold motor units to experimental muscle pain. *J Physiol* 2020.

Martinez-Valdes E, Negro F, Laine CM, Falla D, Mayer F, and Farina D. Tracking motor units longitudinally across experimental sessions with high-density surface electromyography. *J Physiol* 595: 1479-1496, 2017b.

McKenna MJ, Bangsbo J, and Renaud JM. Muscle K+, Na+, and Cl disturbances and Na+-K+ pump inactivation: implications for fatigue. *J Appl Physiol (1985)* 104: 288-295, 2008.

McManus L, Hu X, Rymer WZ, Suresh NL, and Lowery MM. Muscle fatigue increases beta-band coherence between the firing times of simultaneously active motor units in the first dorsal interosseous muscle. *J Neurophysiol* 115: 2830-2839, 2016.

McNeil CJ, Giesebrecht S, Gandevia SC, and Taylor JL. Behaviour of the motoneurone pool in a fatiguing submaximal contraction. *J Physiol* 589: 3533-3544, 2011.

Mettler JA, and Griffin L. Muscular endurance training and motor unit firing patterns during fatigue. *Exp Brain Res* 234: 267-276, 2016.

Mottram CJ, Jakobi JM, Semmler JG, and Enoka RM. Motor-unit activity differs with load type during a fatiguing contraction. *J Neurophysiol* 93: 1381-1392, 2005.

Muceli S, Poppendieck W, Negro F, Yoshida K, Hoffmann KP, Butler JE, Gandevia SC, and Farina D. Accurate and representative decoding of the neural drive to muscles in humans with multi-channel intramuscular thin-film electrodes. *J Physiol* 593: 3789-3804, 2015.

Nawab SH, Wotiz RP, and De Luca CJ. Decomposition of indwelling EMG signals. *J Appl Physiol (1985)* 105: 700-710, 2008.

Negro F, Holobar A, and Farina D. Fluctuations in isometric muscle force can be described by one linear projection of low-frequency components of motor unit discharge rates. *J Physiol* 587: 5925-5938, 2009.

Negro F, Muceli S, Castronovo AM, Holobar A, and Farina D. Multi-channel intramuscular and surface EMG decomposition by convolutive blind source separation. *J Neural Eng* 13: 026027, 2016.

Negro F, and Orizio C. Robust estimation of average twitch contraction forces of populations of motor units in humans. *J Electromyogr Kinesiol* 37: 132-140, 2017.

Pascoe MA, Holmes MR, Stuart DG, and Enoka RM. Discharge characteristics of motor units during long-duration contractions. *Exp Physiol* 99: 1387-1398, 2014.

Riley ZA, Maerz AH, Litsey JC, and Enoka RM. Motor unit recruitment in human biceps brachii during sustained voluntary contractions. *J Physiol* 586: 2183-2193, 2008.

Sacco P, Thickbroom GW, Thompson ML, and Mastaglia FL. Changes in corticomotor excitation and inhibition during prolonged submaximal muscle contractions. *Muscle Nerve* 20: 1158-1166, 1997.

Sawczuk A, Powers RK, and Binder MD. Spike frequency adaptation studied in hypoglossal motoneurons of the rat. *J Neurophysiol* 73: 1799-1810, 1995.

Sogaard K, Gandevia SC, Todd G, Petersen NT, and Taylor JL. The effect of sustained low-intensity contractions on supraspinal fatigue in human elbow flexor muscles. *J Physiol* 573: 511-523, 2006.

Taylor JL, Amann M, Duchateau J, Meeusen R, and Rice CL. Neural Contributions to Muscle Fatigue: From the Brain to the Muscle and Back Again. *Med Sci Sports Exerc* 48: 2294-2306, 2016.

672 **Taylor JL, Butler JE, Allen GM, and Gandevia SC**. Changes in motor cortical excitability during human
673 muscle fatigue. *J Physiol* 490 (Pt 2): 519-528, 1996.
674 **Tenan MS, Marti CN, and Griffin L**. Motor unit discharge rate is correlated within individuals: a case for
675 multilevel model statistical analysis. *J Electromyogr Kinesiol* 24: 917-922, 2014.
676 **Thompson CK, Negro F, Johnson MD, Holmes MR, McPherson LM, Powers RK, Farina D, and Heckman**
677 **CJ**. Robust and accurate decoding of motoneuron behaviour and prediction of the resulting force output.
678 *J Physiol* 596: 2643-2659, 2018.
679 **Thorstensen JR, Taylor JL, Tucker MG, and Kavanagh JJ**. Enhanced serotonin availability amplifies
680 fatigue perception and modulates the TMS-induced silent period during sustained low-intensity elbow
681 flexions. *J Physiol* 598: 2685-2701, 2020.
682 **Vila-Cha C, Falla D, Correia MV, and Farina D**. Adjustments in motor unit properties during fatiguing
683 contractions after training. *Med Sci Sports Exerc* 44: 616-624, 2012.

684

685

686

687 **FIGURE CAPTIONS**

688 **Figure 1. Procedure for motor unit tracking during sustained-submaximal fatiguing contractions.**

689 A knee extension contraction at 30% of the maximal voluntary torque (MVC) until failure is shown from
690 a representative subject. Surface EMG and torque signals were cut into 30s segments (blue and orange
691 arrows) overlapped by 15s. Surface EMG signals from each of these segments was then decomposed
692 independently to reveal the firing activity of individual motor units (MU). Overlapped segments were
693 then used to cross-correlate MU spike trains from each 30s-segment identified MU and then merged to
694 reconstruct the activity of individual MU throughout the contraction. In addition to this, twitch force
695 was also estimated from the active motor units (fused twitches) in 5 segments corresponding to 20, 40,
696 60, 80 and 100% of total endurance time.

697 **Figure 2. Spatial 2D Cross-correlation of motor unit action potentials (MUAPs)**

The 50 initial (beginning, blue) and 50 final (task failure, red) firings belonging to each tracked motor unit were used to trigger HDsEMG signals to build the 2D spatial representation of MUAPs (59 bipolar channels). These MUAPs were then matched by cross correlation (above the figure). Note the increase in MUAP amplitude and length at task failure.

Figure 3. Representative motor unit firing behaviour of vastus medialis (VM) from one participant.

Firing behaviour of tracked motor units (coloured lines) and torque signal (black line, 30% of the maximum voluntary contraction torque, MVC) are presented in 1s epochs. 16 motor units were identified during the course of the contraction and 10 motor units could be followed once the target was reached (30% MVC) until failure. These 10 motor units had an average recruitment threshold of 21.0% MVC. The first active motor units (blue and red lines) were recruited at 7.3% and 13.4% MVC respectively. Regardless of when the motor units were recruited, they all follow the same behaviour of the earlier recruited ones, that is, they decrease discharge rate until 60s of the contraction (motor unit behaviour reversal point) and then increase discharge rate from 60s of the contraction until task failure. Two motor units were recruited before the motor unit behaviour reversal point and four additional motor units were recruited after the motor unit behaviour reversal point. Note the common oscillations between motor unit discharge rate and the torque signal.

Figure 4. Motor unit non-linear firing behaviour from the full group of participants

Instantaneous discharge rate from early-recruited motor units was averaged for each participant (1s windows) during the sustained contraction for vastus medialis and vastus lateralis. 13 out of the 14 participants showed a nonlinear behaviour in DR, where firing frequency decreased and then increased at a certain point during the contraction. Only one participant depicted in bright green, showed a linear decrease in DR.

Figure 5. Motor unit firing properties, torque and cross-correlation of firing times and torque

Changes in discharge rate (A), coefficient of variation for the interspike interval (CoVisi, B), coefficient of variation of Torque (CoV Torque, C) and cross-correlation between fluctuations in torque and discharge rate of single motor units (D) is presented for the group of participants in vastus medialis and lateralis (VM and VL, respectively). Data was normalized according to total endurance time in 10 epochs. Significant decrease from baseline, Ψp<0.05). Significant increase from baseline, #p<0.05 and *p<0.01.

Figure 6. Discharge rate, interspike interval variability and torque variability breakpoints.

Reversal points in discharge rate (DR) (A), coefficient of variation for the inter-spike interval (CoVisi) (B) and coefficient of variation of torque (CoV torque) (C), are presented for one representative participant's vastus medialis and lateralis (VM and VL) muscles. Data represent the average behaviour of 3 VM and 3 VL motor units that could be tracked from target torque until failure. Data is averaged in 1s epochs which were fitted by bi-linear regression (piecewise regression). The point in time where the regression lines intersected was used as a breakpoint to mark the change in motor unit firing and torque behaviour. The breakpoint in VM and VL discharge rate, CoVisi and CoV torque happened at a similar time during the contraction (range: 77.5s to 81.5s).

Figure 7. Correlation between motor unit behaviour reversal point and endurance time.

As reversal points in discharge rate, coefficient of variation for the inter-spike interval (CoVisi) and coefficient of variation of torque (CoV torque) happened at similar time instants. Their values were averaged to represent a single point during the contraction. This specific time-instant was called motor unit behaviour reversal point and was able to predict the time to task failure.

Figure 8. Discharge rate for the same motor unit identified during a non-fatiguing 50% MVC contraction and a 30% MVC contraction at task failure

A VL motor unit identified during the non-fatiguing 50% MVC contraction was tracked at task failure (30% MVC) by cross-correlation of the 2D-spatial MUAPs (59 bipolar channels). Despite of the increase in discharge rate at task failure with respect to the beginning of the contraction (30% MVC, figure 6A), discharge rate for this unit did not reach the firing frequency observed during a non-fatiguing 50% MVC contraction.

Figure 9. Differences in discharge rate for motor units that were tracked during 50% MVC and 30% MVC at task failure

Differences in discharge rate between 50% MVC and discharge rate at task failure for early (active from the beginning of the 30% contraction, A) and late (active at the end or close to the end of the 30% MVC contraction, B) recruited motor units for VM and VL muscles during the 30% MVC contraction. Significant effect of force, *$p<0.001$. Significant effect of recruitment (early vs late), #$p<0.01$.

Figure 10. Interference EMG

Changes in root mean square amplitude of interference EMG signal averaged across 59 bipolar channels is presented for the group of participants for the vastus medialis and lateralis (VM and VL, respectively). A) Data was normalized according to total endurance time in 10 epochs. B) RMS values are compared between 50% MVC and 30% MVC at task failure (TF). Significant interaction between muscles, *$p<0.001$. Main effect of time, #$p<0.05$.

Figure 11. Changes in vastus medialis twitch force during the course of the contraction

Twitch force results and its relation with discharge rate from one representative subject are shown in the figure. Twitch areas are expressed in arbitrary units (AU).

SEMG

Fused MU twitch forces

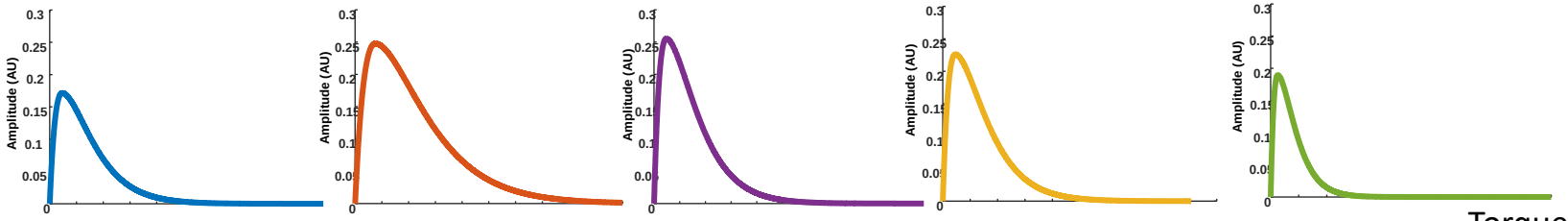

Torque (30% MVC)

15 s

30 s

30 s

30 s

30 s

30 s

30 s

30 s

MU Spike train

...

Time (s)

CROSS-CORRELATION

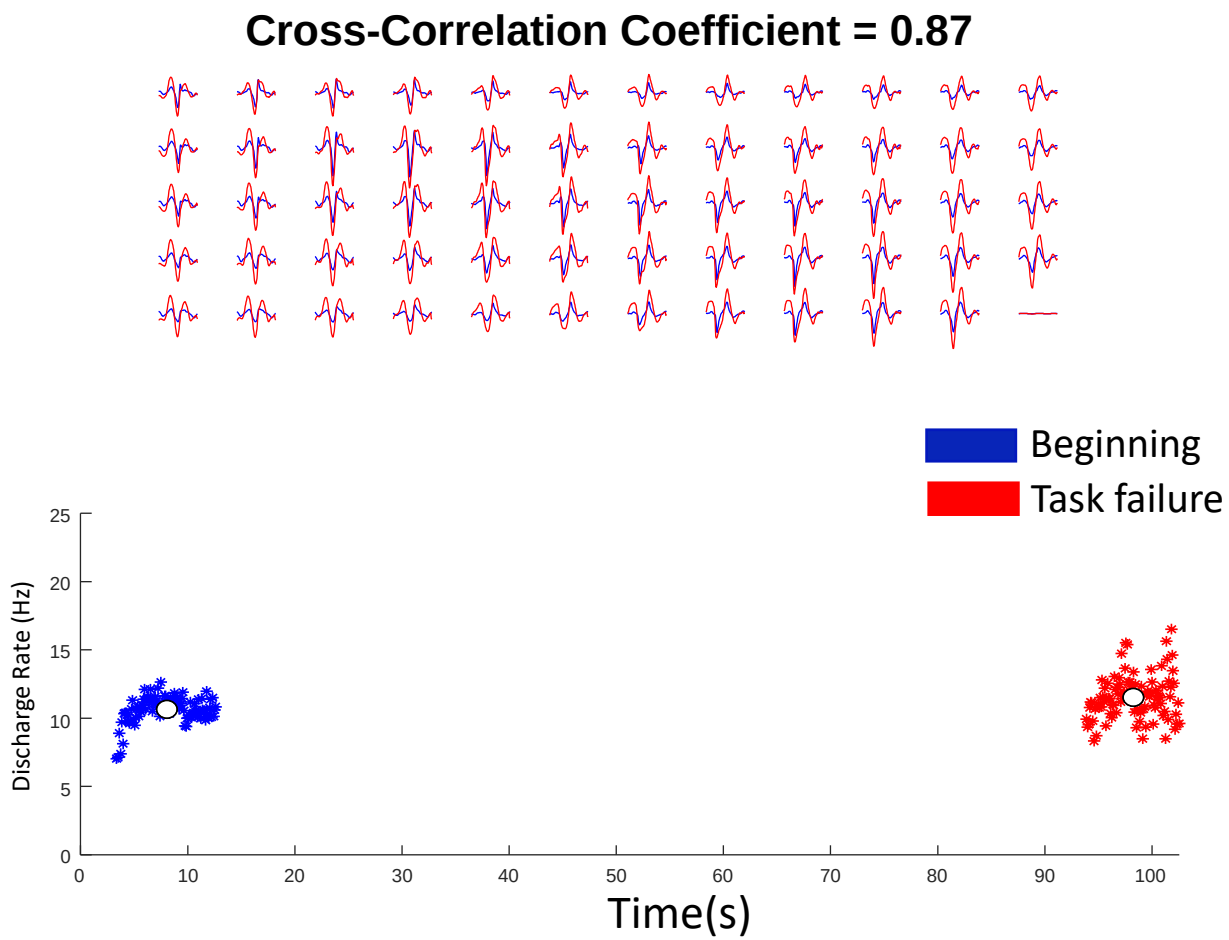
Cross-Correlation Coefficient = 0.87
Beginning
Task failure
Discharge Rate (Hz)
0
5
10
15
20
25
0
10
20
30
40
50
60
70
80
90
100
Time(s)

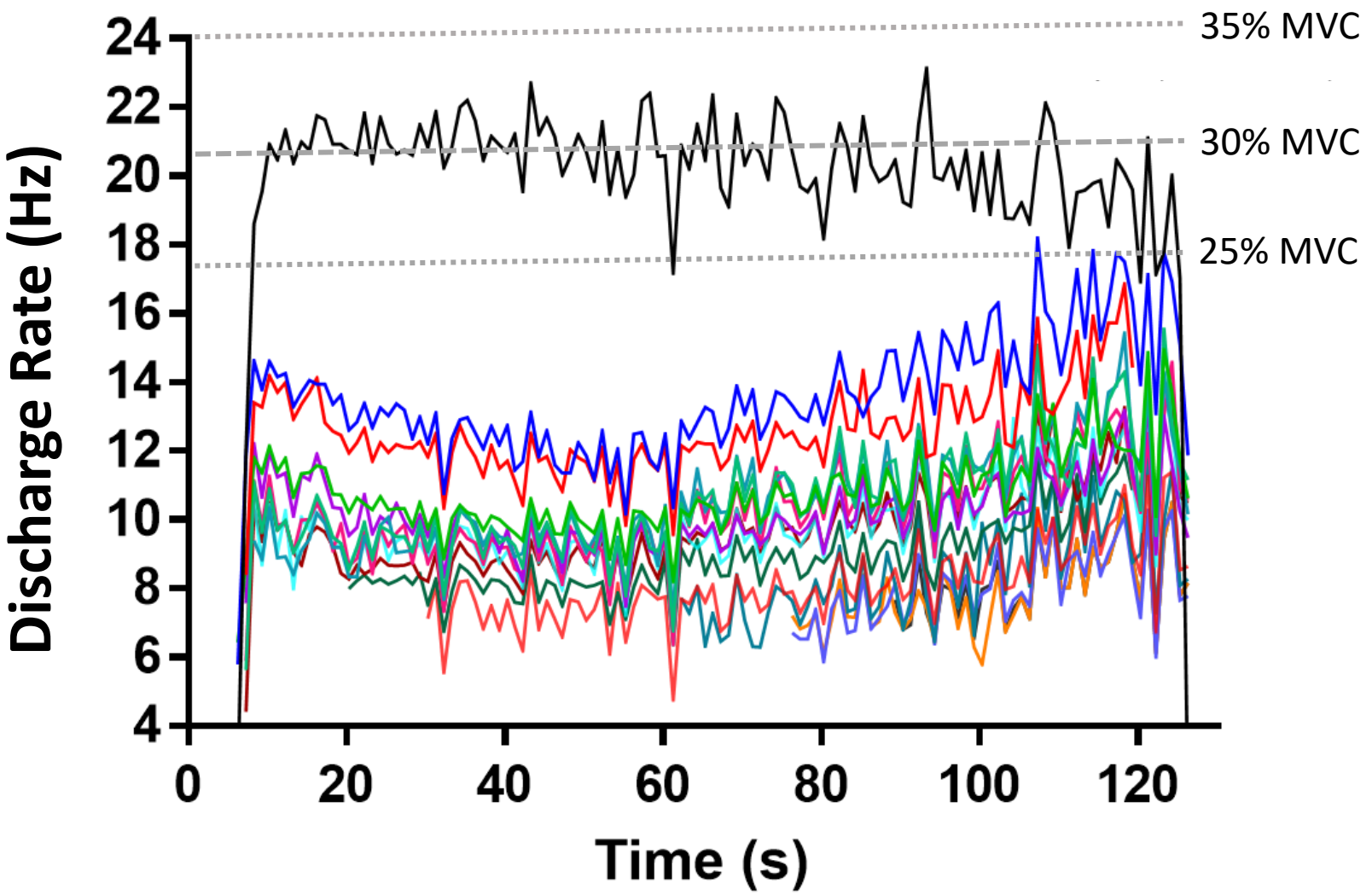
35% MVC
30% MVC
25% MVC
Discharge Rate (Hz)
24
22
20
18
16
14
12
10
8
6
4
0
20
40
60
80
100
120
Time (s)

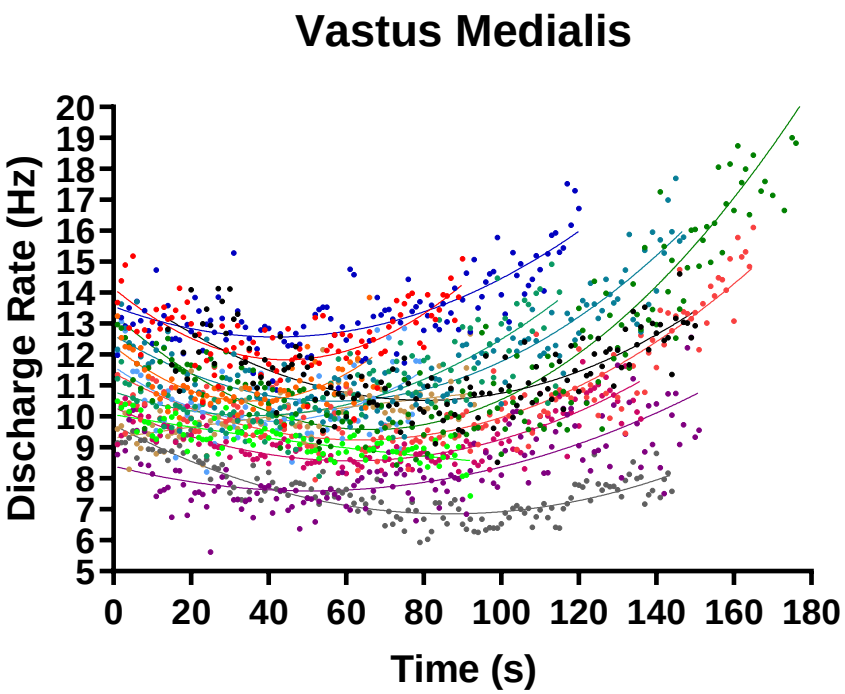
Vastus Medialis
Discharge Rate (Hz)
20
19
18
17
16
15
14
13
12
11
10
9
8
7
6
5
0
20
40
60
80
100
120
140
160
180
Time (s)

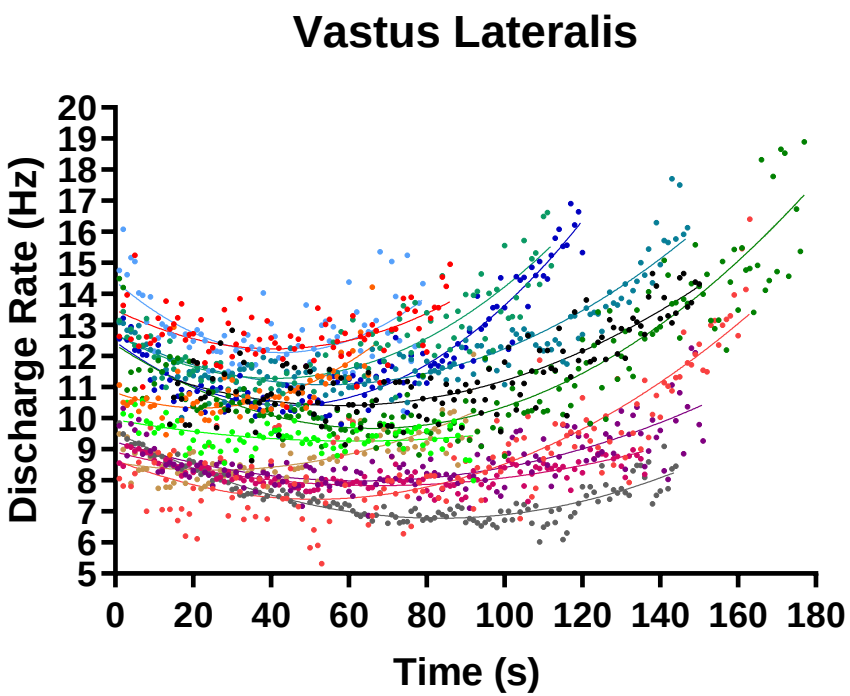
Vastus Lateralis
Discharge Rate (Hz)
20
19
18
17
16
15
14
13
12
11
10
9
8
7
6
5
0
20
40
60
80
100
120
140
160
180
Time (s)

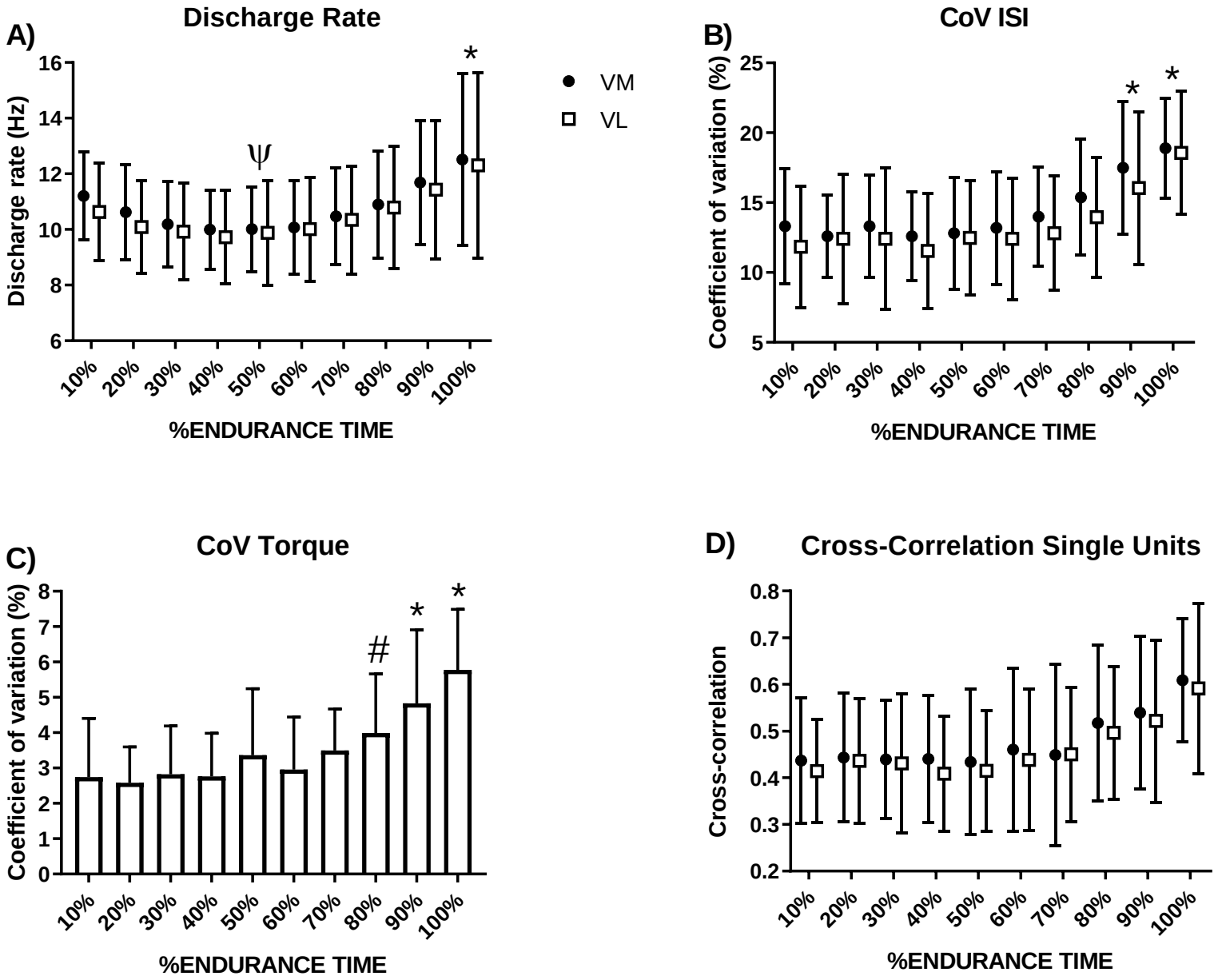
A)
Discharge Rate
Discharge rate (Hz)
16
14
12
10
8
6
ψ
*
VM
VL
10%
20%
30%
40%
50%
60%
70%
80%
90%
100%
%ENDURANCE TIME
B)
CoV ISI
Coefficient of variation (%)
25
20
15
10
5
*
*
%ENDURANCE TIME
C)
CoV Torque
Coefficient of variation (%)
8
7
6
5
4
3
2
1
0
#
*
*
%ENDURANCE TIME
D)
Cross-Correlation Single Units
Cross-correlation
0.8
0.7
0.6
0.5
0.4
0.3
0.2
%ENDURANCE TIME

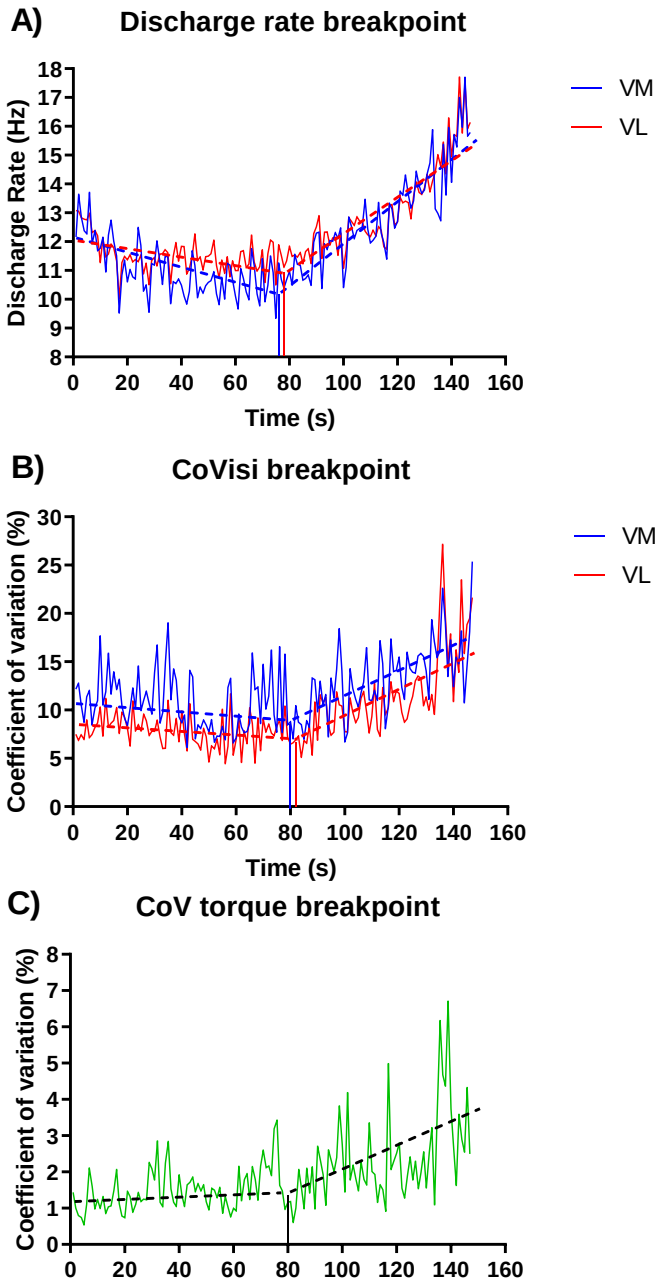
A)
Discharge rate breakpoint
Discharge Rate (Hz)
Time (s)
VM
VL
B)
CoVisi breakpoint
Coefficient of variation (%)
Time (s)
VM
VL
C)
CoV torque breakpoint
Coefficient of variation (%)

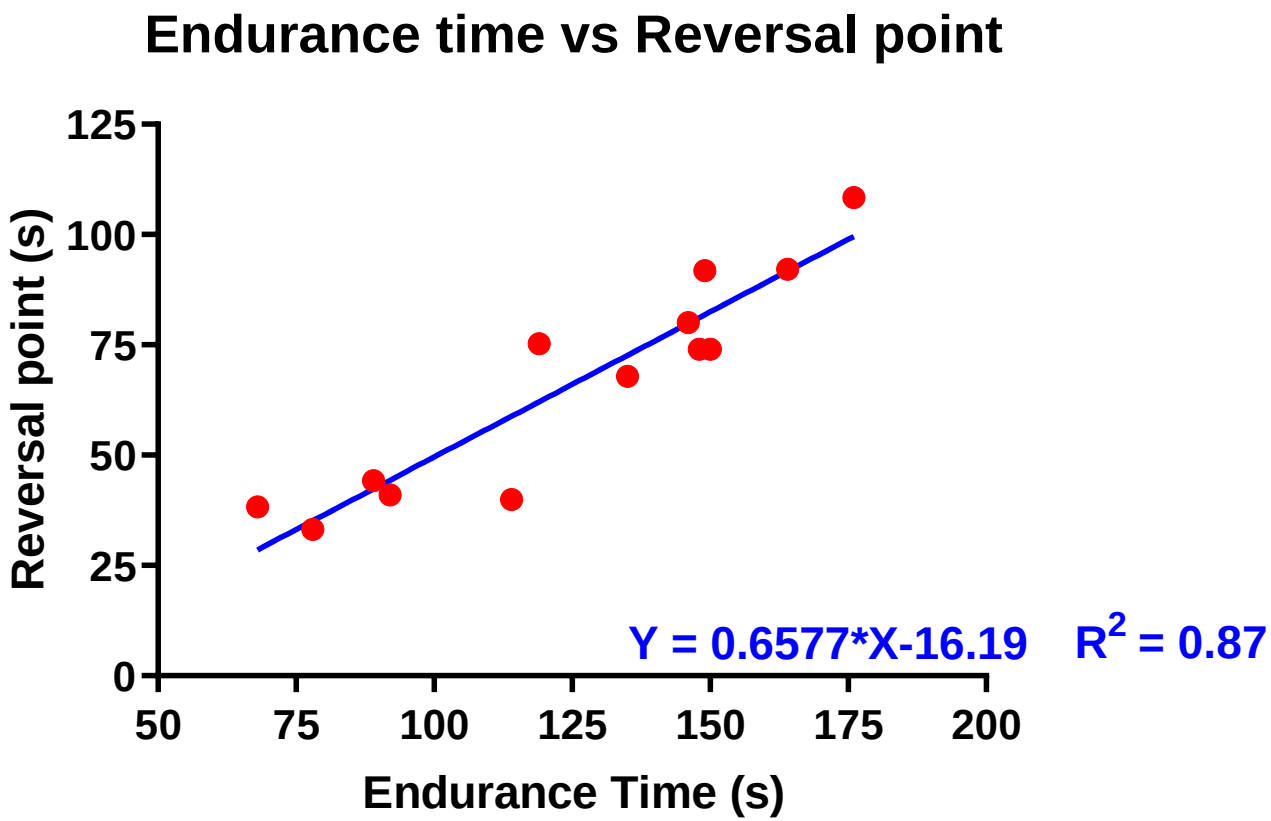
Endurance time vs Reversal point
Reversal point (s)
125
100
75
50
25
0
50
75
100
125
150
175
200
Endurance Time (s)
Y = 0.6577*X-16.19
R2 = 0.87

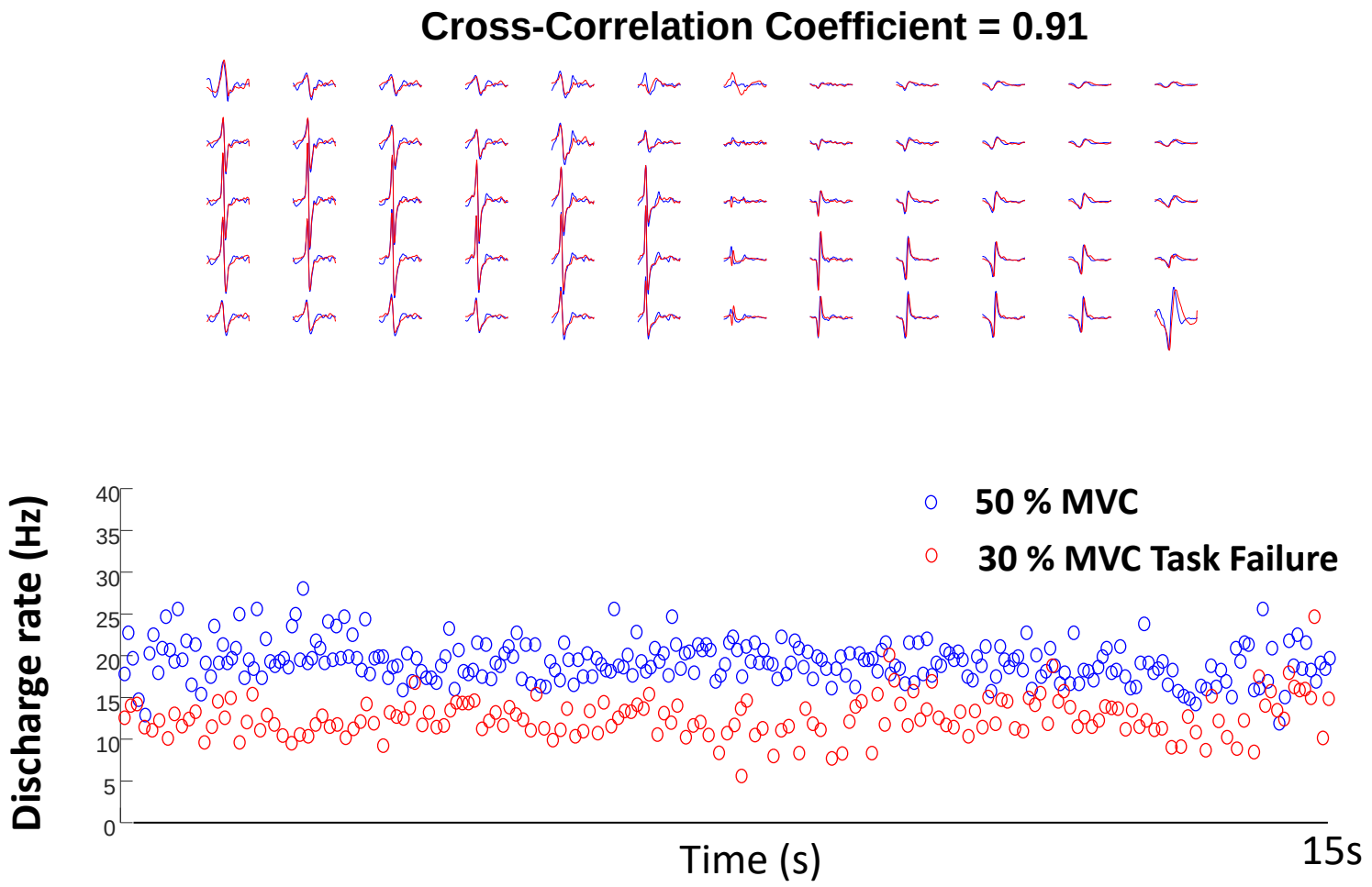
Cross-Correlation Coefficient = 0.91
Discharge rate (Hz)
40
35
30
25
20
15
10
5
0
50 % MVC
30 % MVC Task Failure
Time (s)
15s

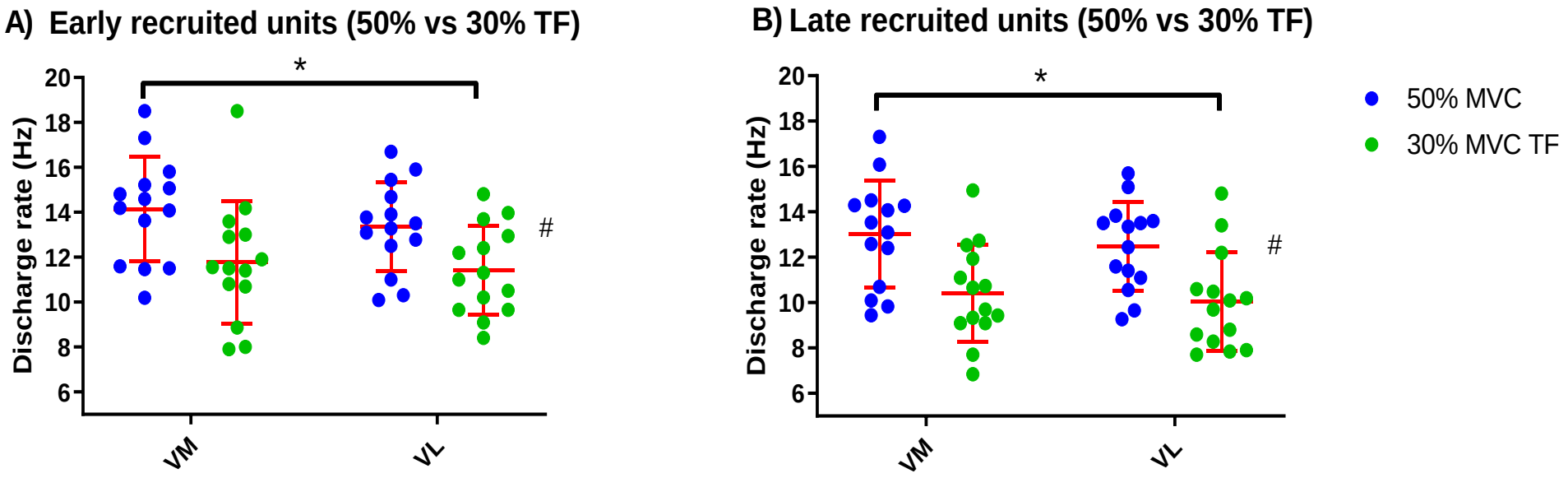
A) Early recruited units (50% vs 30% TF)
B) Late recruited units (50% vs 30% TF)
Discharge rate (Hz)
20
18
16
14
12
10
8
6
*
#
VM
VL
50% MVC
30% MVC TF

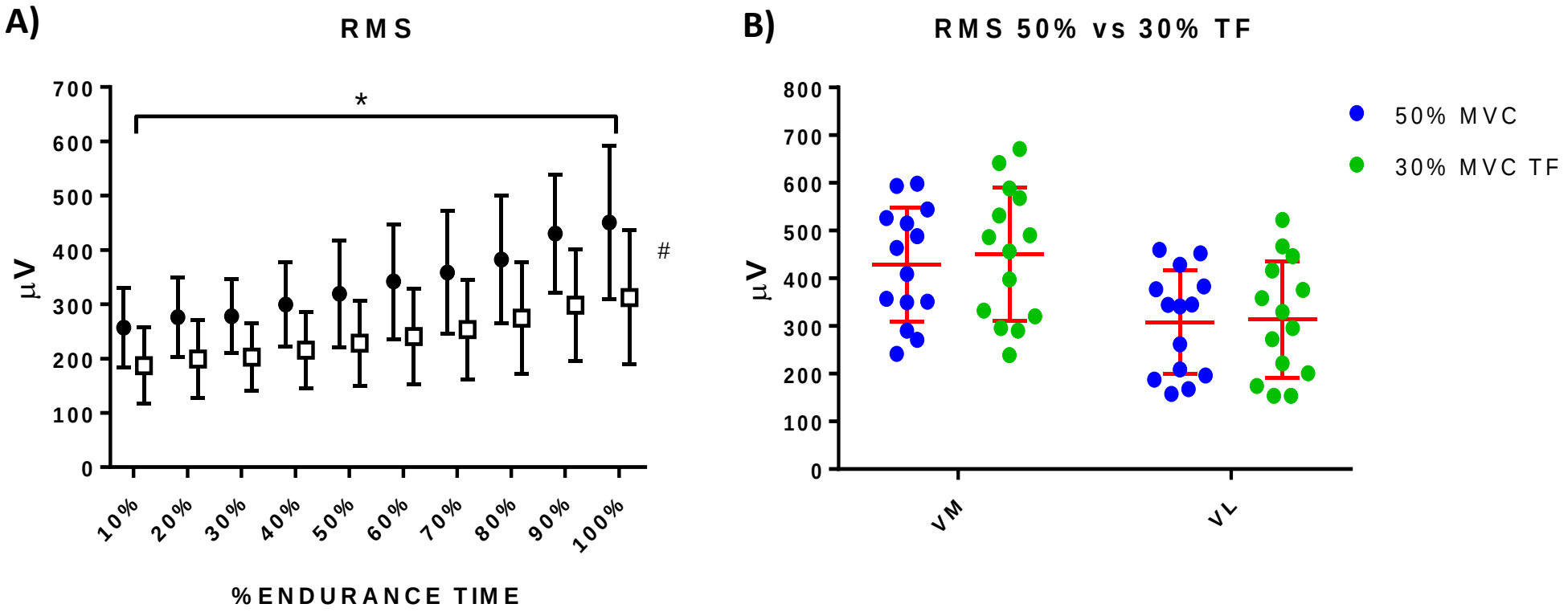
A)
RMS
700
600
500
400
300
200
100
0
µV
*
#
10%
20%
30%
40%
50%
60%
70%
80%
90%
100%
%ENDURANCE TIME
B)
RMS 50% vs 30% TF
800
700
600
500
400
300
200
100
0
µV
VM
VL
50% MVC
30% MVC TF

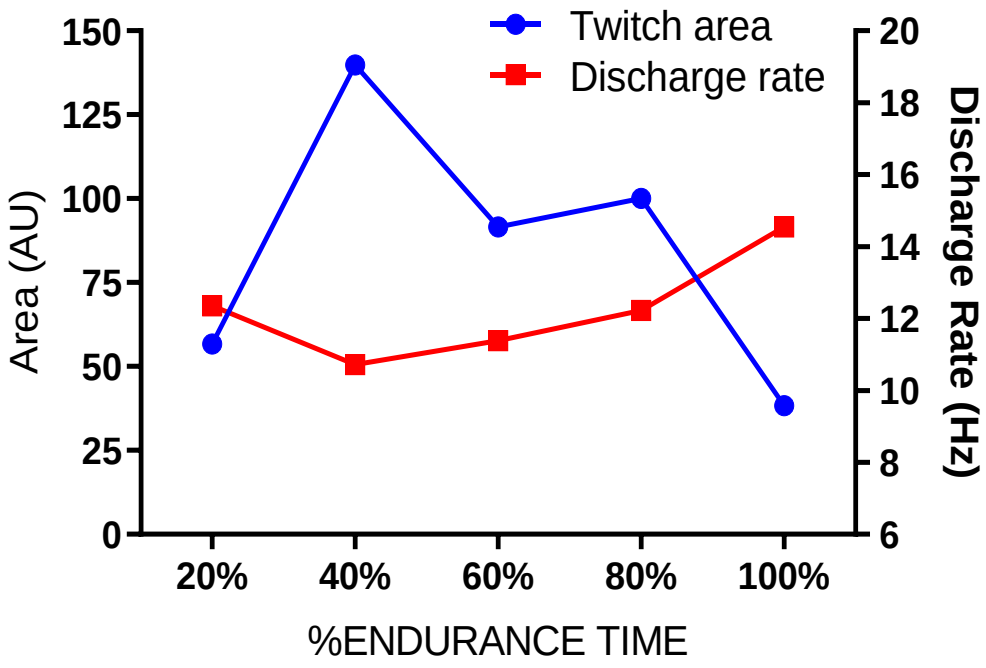
Twitch area
Discharge rate
Area (AU)
Discharge Rate (Hz)
150
125
100
75
50
25
0
20
18
16
14
12
10
8
6
20%
40%
60%
80%
100%
%ENDURANCE TIME